SEMARAK ILMU PUBLISHING

Journal of Advanced Research in Micro and Nano Engineering

Journal homepage:
https://semarakilmu.com.my/journals/index.php/micro_nano_engineering/index
ISSN: 2756-8210

Effect of Adding Al_2O_3 Ceramic in Wire Arc Additive Manufacturing 308LSi Stainless Steel

Mohd Hairizal Osman[1,3,*], Mohd Rizal Alkahari[1,3], Lailatul Harina Paijan[2], Dzuraidah Abd Wahab[4]

[1] Faculty of Mechanical Engineering, Universiti Teknikal Malaysia Melaka, Hang Tuah Jaya, 76100 Durian Tunggal, Melaka, Malaysia
[2] Faculty of Mechanical and Manufacturing Engineering Technology, Universiti Teknikal Malaysia Melaka, Hang Tuah Jaya, 76100 Durian Tunggal, Melaka, Malaysia
[3] Center for Advanced Research on Energy (CARE), Universiti Teknikal Malaysia Melaka, Hang Tuah Jaya, 76100 Durian Tunggal, Melaka, Malaysia
[4] Department of Mechanical and Manufacturing Engineering, Faculty of Engineering and Built Environment, Universiti Kebangsaan Malaysia, 43600 Bangi, Selangor, Malaysia

ARTICLE INFO

Article history:
Received 2 August 2024
Received in revised form 9 September 2024
Accepted 18 October 2024
Available online 30 November 2024

Keywords:
Wire arc additive manufacturing; Al_2O_3 ceramics particles; 308LSi; mechanical properties; grain refinement; microstructure

ABSTRACT

Wire Arc Additive Manufacturing (WAAM) is a process that allows for efficient in-situ production of components or remanufacturing based on its capabilities to produce at a greater rate of deposition at a lower cost. However, WAAM components suffer from heat dissipation during the deposition process that causes the growth of coarse columnar grains resulting in poor mechanical properties that will limit industrial applications. Thus, this research investigates the role of introducing Al_2O_3 ceramic powder particle inoculants to the AWS A5.9 ER308LSi stainless steel wall structure to enhance the mechanical performance capabilities by refining the grain process. During deposition, the Al_2O_3 ceramic powder particle was manually added to each layer when the temperature drops to 150°C. A complete series of tensile testing was executed to bridge those knowledge gaps. WAAM walls were fabricated and the microstructure of the sample were analysed. The results revealed that the highest tensile strength of WAAM SS308LSi components recorded at 560 MPa in the deposition direction, which increased by 6% compared to the non-inoculated sample. The improvement was due to the success of grain refinement and heterogeneous nucleation. The study demonstrates the potential of the technique to improve the mechanical properties and microstructure during WAAM components fabrication or remanufacturing.

1. Introduction

Additive manufacturing (AM) is well-defined as a component fabricating material usually layer upon layer process for building components to create objects from 3D model data where the raw materials can be in the form of liquid or solid (sheet, powders or wires) as feedstock, melted in a controlled parameter and finally cooled to form a component [1,2]. AM has been categorized into seven categories by the American Society for Testing and Materials (ASTM) namely powder bed fusion, material extrusion, material jetting, binder jetting, material extrusion, sheet lamination, VAT

* *Corresponding author.*
E-mail address: hairizal@utem.edu.my

https://doi.org/10.37934/armne.27.1.133145

photopolymerization and directed energy deposition (DED) [3-5]. Among other several AM techniques, Wire Arc Additive Manufacturing (WAAM) is one of the DED process variants that use welding processes such as plasma arc welding (PAW), tungsten inert gas (TIG) and metal inert gas (MIG) as an energy source to deposit input material to build metallic components [6]. WAAM is a lower-cost technique when compared to other existing AM processes due to the raw material obtainable via the feeding system of commercial welding for layer-by-layer buildup until the multi-dimensional part is accomplished. Furthermore, WAAM offers convincing benefits regarding high forming efficiency, low capital fabrication costs and also probable application in the deposited of larger parts [7]. Due to these benefits and its flexibility, WAAM is an ideal solution and potential process for parts repair and restoration in remanufacturing.

Remanufacturing is restoring used products into new ones through cleaning, repairing and refurbishing through a systematic process to ensure the quality, performance and aesthetics are comparable to the original products, including their warranty. With the advent of AM, it is highly potential for WAAM to be deployed in remanufacturing repair and restoration. During remanufacturing, WAAM is used to add more material to the original material at the outer layer. Hence, it has the potential to enhance the mechanical properties of remanufactured parts and components of machine tools, mold and die, piping equipment, automotive and aircraft components.

WAAM is extensively deployed in the deposition of alloys and metallic materials such as stainless steel, aluminum and titanium. It has been widely applied in oil & gas, aeronautics, automotive, nuclear and naval fields [8,9]. However, coarse grain structure and columnar crystal epitaxial development were causing the effects of mechanical deterioration during WAAM formation [10]. As a result, fine grains with uniform microstructures generated by WAAM are highly desirable. Epitaxial formation with large grains within layers may result in poor and extremely anisotropic mechanical characteristics inside the deposited structure due to rapid solidification and continual thermal accumulation of built-up components during the deposition process which restricts the application in industries [11,12]. A conceivable approach to avoid material softening is to increase dwell time among repeated deposited layers in order to lower the heat accumulated at higher temperatures.

However, in a competitive industrial context, prolonged dwell duration within layers might be unfavorable to WAAM implementation. Thus, a suitable strategy for lowering grain sizes needs to be imposed to counter a decrease in the hardness of WAAM components. This is accomplished by using inoculating agents to alter the nucleation as well as growth sequences throughout its solidification [13,14]. The introduction of hard ceramic inoculant reinforcement such as TiN [15,16], SiC [13], TiB2 [17] and TiC [18] may assist with grain refinement, hardened precipitation, dense solution strengthening and even material composition modifications [11,19]. Ceramics inoculant addition has recently been identified as an excellent method for refining the structure of grains in the metal-casting industries as well as stimulating the formation of equiaxed grains. Modifying agents are able to be employed as nucleating agents to enhance crystal grain formation, pin grain boundaries and inhibit crystal grain development. As a result, restricting the formation of rough columnar crystals in WAAM components, encouraging the formation of fine equiaxed particles as well as maximizing the performance enhancement impact are necessary to enhance component strength and toughness [10].

Alumina ceramics (Al_2O_3) are potential inoculants due to their excellent level of hardness, wear resilience, physical stability, high-temperature resistance as well as chemically resistant properties. On the other hand, oxide particles such as Al_2O_3 have substantially higher thermal stability than carbides such as TiC, VC and so on [19]. Paul *et al.,* [20] attempted to join stainless steel (SS) 304L as a substrate and aluminum (Al) 4043 wire filler using the Wire arc direct energy deposition (WA-DED) process. The authors revealed that due to the addition of Al_2O_3 ceramic inoculant, the grain

refinement size has become exceedingly fine up to 2µm. As the input current increases, more Al_2O_3 spreads inside the Al-matrix that acts as a grain refiner. They also discovered that the addition of Al_2O_3 ceramic inoculant boosted hardness and strength to 600HV and 77.5MPa, respectively. Kumar *et al.,* [21] investigated the material and vibrational behavior of stainless steel (SS) 304 reinforcing Al_2O_3 microparticles via a tungsten inert gas (TIG) welding and laser welding (LW) technique. They observed recrystallized grain structure at the fusion zone was strongly influenced by adding ceramic inoculant Al_2O_3. It seemed that the grain size in the micro particle-rich area was severely refined.

Despite inoculation being a common practice in metal casting operations, its implementation and effectiveness in WAAM have received the least attention [13]. To the best of our knowledge, the impact of the presence of alumina ceramics (Al_2O_3) on microstructure characteristics as well as mechanical properties of stainless steel (SS) produced via WAAM has been the least studied although it could potentially affect the potential for WAAM deposition process fabrication combined with (DED-MIG) joining method. Therefore, the effect of WAAM method deposition with the potential of an Al_2O_3 inoculation with stainless steel (SS) 308LSi welding wire is investigated in this work. The introduction of Al_2O_3 inoculant refined the microstructure and also resulted in improved mechanical characteristics, respectively. It has significant reference and application value in terms of increasing the performance of WAAM stainless steel thin walls.

2. Methodology

2.1 Deposition Method

In this study, a commercial austenitic stainless-steel grade of AWS A5.9 ER308LSi with a 1.2 mm diameter welding stainless steel wire was deployed as feedstock material for the WAAM process and the chemical composition is depicted in Table 1. A robotic WAAM platform comprised of a KempArc Pulse 350 with a synergic MIG/MAG power source and a 6-axis ABB IRB1410 robotic arm was adopted to deposit wall structures. The printing substrate was AISI 1018 low-carbon steel plate with a thickness of 10mm selected to ensure stable depositions during the WAAM deposition process. Previously, the outer layer of the substrate had been polished with a wire-tipped brush to remove stain on the surface as well as the surface oxidation layer followed by cleaning with alcohol.

Table 1
Chemical composition (wt.%) following EN ISO 14343-2017 [22]

Elements	C	Mn	Si	Cr	Ni	P	S
Composition (wt%)	≥ 0.03	1.50- 2.10	0.65 - 1.00	19.5 - 21.0	9.0 - 11.0	≥0.030	≥0.020

The WAAM was performed using a metal inert gas technique and the ER308LSi was deposited onto a mild steel substrate. In order to introduce alumina oxide (Al_2O_3) into stainless steel structure, 0.560g of alumina powder with particles size 30µm was weighed by an electronic balance and mixed with an alcohol-based solvent uniformly before it was added to the top surface of each deposited layer to form a thin coating. Then, the alumina adhered to the deposited substrate after the solvent evaporated and was absorbed into the melted pool due to the subsequently deposited layer using standard WAAM parameter setup as depicted in Table 2. The effect of the WAAM structure coated with Al_2O_3 suspension was compared to that of a non-inoculated Al_2O_3 WAAM sample.

Table 2
Process parameter of WAAM deposition process

Process parameter	Value
Wire feed speed (WFS) (m/s)	8 m/s
Travel speed (mm/s)	6 mm/s
Voltage (V)	19 V
Electrode to layer angle	138A
Welding wire	90°
Wire diameter	ER308LSi
Shielding gas	1.2mm
Gas flow rate	20L/min
Interlayer temperature	150°C

Furthermore, the procedure involves pauses among layers to enable the substance to cool down until it exceeds an interpass temperature of less than 150°C without the use of external cooling. The temperature of the previous layer was checked by a Fluke Ti451 thermographic infrared camera. The infrared camera stands 900 meters away from the welding robot. Each deposition layer was established by positioning a welding torch in an upward direction while performing zig-zag deposition path strategies as depicted in Figure 1 while wires were fed into the molten pool. From repeated deposition and coating, an ER308LSi stainless steel thin-walled wall component with a length of 280 mm and a height of 60 mm was developed.

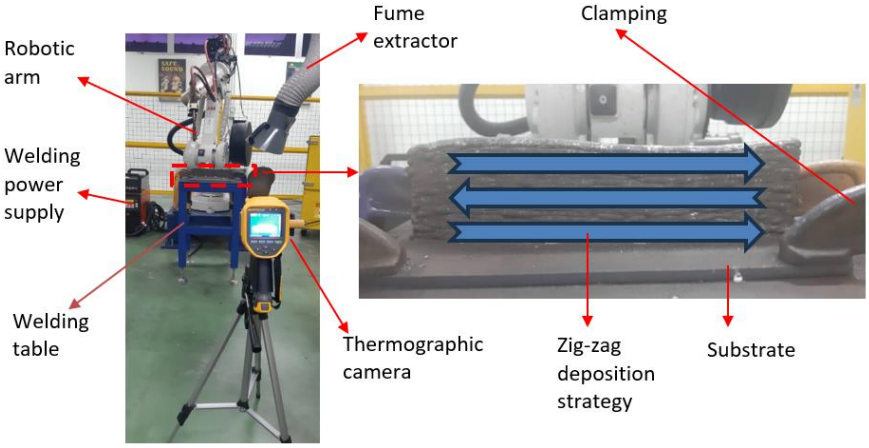

Fig. 1. WAAM experimental setup

The flow diagram of the preparation sample and deposition process of this experiment is shown in Figure 2.

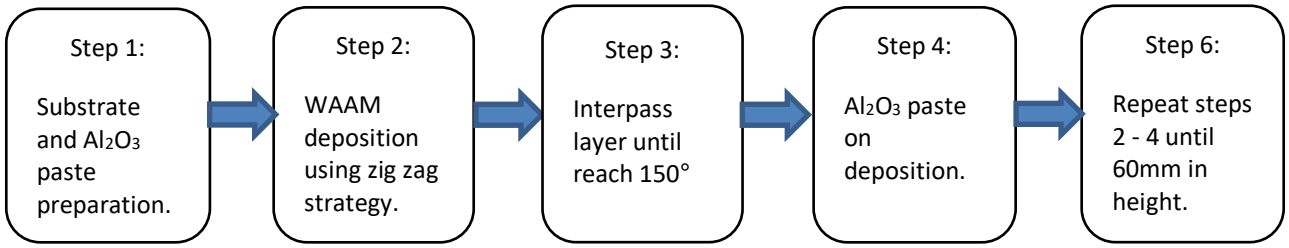

Fig. 2. Flow diagram of the prepared sample and deposition process of Al_2O_3 ceramics inoculant particles on the ER308LSi austenitic stainless steel

All the experimental specimen samples are shown in Figure 3.

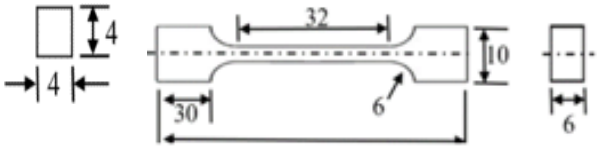

(a) (b)

Fig. 3. Illustration of WAAM sample (a) dimensions of a metallographic specimen (b) specimens' dimensions of the tensile test

2.2 Metallography Analysis

For metallography analysis, samples have been sliced at cross-sectional sections of the WAAM following the building direction and the sample size is illustrated in Figure 3(a). The sample was encased in a plastic shell molding for easier grasp and stability using an automatic mounting metallography press machine (Ecopress 100). The surface was then polished using 800 - 2000 grit abrasive grinding papers until it was free of scratches. Subsequently, the sample's surface was polished using a polishing machine (PRESI MECAPOL P320) with a polishing pad size 6µ and 3µ with DIAMAT polycrystalline diamond polishing agent to form a smooth reflect surface. Then, the sample was etched for 30 seconds with a mixture of 110 ml hydrochloric acid, 12 ml nitric acid and 119 ml distilled water and immediately rinsed thoroughly under running water.

The microstructure and fracture morphology components were analyzed using a metallurgical optical microscope (Nikon LV100) and scanning electron microscope (SEM, JEOL JSM-6010PLUS/LV) to analyze the microstructural WAAM deposited wall of non-inoculated and inoculant Al_2O_3 ceramic particles, respectively. The sample element content was determined using the SEM's energy-dispersive spectroscopy (EDS) probe (Oxford EDS detector) to examine the element content of the WAAM wall deposited structure.

After deposition processing, three samples (bottom, middle and top) for mechanical properties for both non-inoculated and inoculant Al_2O_3 ceramic particles were extracted using wire electrical discharge machining (Sodick VZ300L) and then evaluated using Universal Testing Machine (Shimadzu Autograph AG100 KNG). ASTM-E8M standard was referred to for purposes of cutting tensile samples as displayed in Figure 3(b). Each of the experiments was carried out at 26.0°C room temperature and 63% humidity, respectively. The yield strength was calculated using the recorded stress-strain curve and tested at a rate of 0.08 mm/s. Three specimens were tested and the average results are shown throughout the graph. Scanning Electron Microscopy (SEM) was used to examine the fracture microstructure of materials.

3. Results

3.1 Microscopic Characterization

Initially, an EDS test was conducted to assure the penetration of Al_2O_3 element ceramic powder particle into the layers during the deposition of WAAM structure as depicted in Figure 4(a). From the result, it was revealed that the presence of Al_2O_3 element was magnificently infiltrated into the WAAM structure sample with a 0.4 % of Al_2O_3, respectively as depicted in Figure 4(b). In other words, the existence of the Al_2O_3 ceramic particles content element in WAAM structure was achieved with its introduction inside the melting pool throughout the process of deposition.

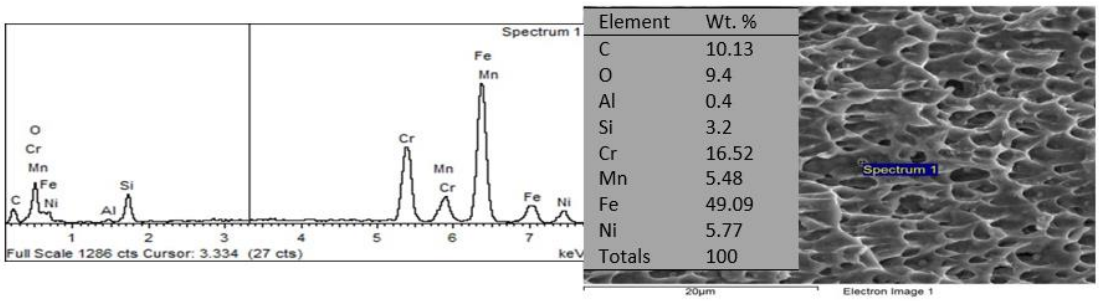

(a) (b)

Fig. 4. EDS analysis results for inclusion of WAAM wall structure (a) EDS spectrum of Al_2O_3 inoculated inclusion (b) Inoculated inclusion view

For the purposes of investigating the characteristics of deposition components, the surface morphology of WAAM components can be examined by investigating metallographic images of specimens. With the deposition using SS308LSi filler wire, two types of phase morphology in wall components such as γ-austenite and δ-ferrites remain in the austenite boundary matrix. Due to the influence of the remelting heat on the subsequent layers, the bonding zone is partially dissolved in austenite, while a mesh structure eventually develops from the remaining δ-ferrites in the WAAM structure [37]. During the lowering of temperature, the complete process leaves the ferrite-to-austenite transformation. Through the cooling process, the smaller ferrite particles are entirely altered to austenite, however, larger primary dendrites are unable to be dissolved completely thus generating a skeletal coarse columnar ferrite that produced coarse dendrites in the final microstructure as depicted in Figure 5(a). Furthermore, the presence of δ-ferrites is essential for austenitic stainless steel since ferrite content reduces undesirable metallurgical changes and weld defects such as hot cracking, embrittlement and corrosion resistance from occurring and is very beneficial used in mining, oil and gas and also in shipbuilding industries where there are under extreme operating conditions [23]. However, the existence of excess δ-ferrites will enhance the susceptibility impacts of various metallurgical and mechanical properties at elevated temperatures [24]. Moreover, the presence of microstructure is also reported in coarse dendrites which develop nearly in the vertical orientation due to the accumulation of heat input that occurs during repeated heating and cooling, heat removal rate perpendicular to the fusion line and high-temperature gradients is higher as well during the deposition process [10]. The result also agrees with Koli *et al.,* [23] that the coarser columnar dendrites occurred owing to thermal accumulation in between layers, which leads to a coarser grain structure.

However, inoculated WAAM components containing inoculant Al_2O_3 ceramic particles produced a smaller grain structure as depicted in Figure 5(b). The result revealed that the effect of grain refining improves after the addition of inoculant Al_2O_3 ceramic particles as compared with non-inoculant grains. Furthermore, the introduction of inoculant Al_2O_3 ceramic particles was essential in generating a finer dendritic structure of components. The inoculant is responsible for pinning the grain borders, dragging the grain boundaries, delaying grain boundary growth, hindering grain growth as well as refining the grains. It also has the potential to be employed as a nucleating agent to promote crystal grain nucleation, which results in a more uniform and refined grain structure. It can also be used as a nucleating agent to stimulate crystal grain nucleation, resulting in a uniform and refined grain structure [10]. This is supported by a study from Li *et al.,* [25] who achieved smaller grain sizes of cast AZ91 alloys after the addition of Al_2O_3 ceramic nanoparticles even if the cooling rate is higher than 90 K/s. The authors also concluded that nanoparticles can effectively promote finer grain size.

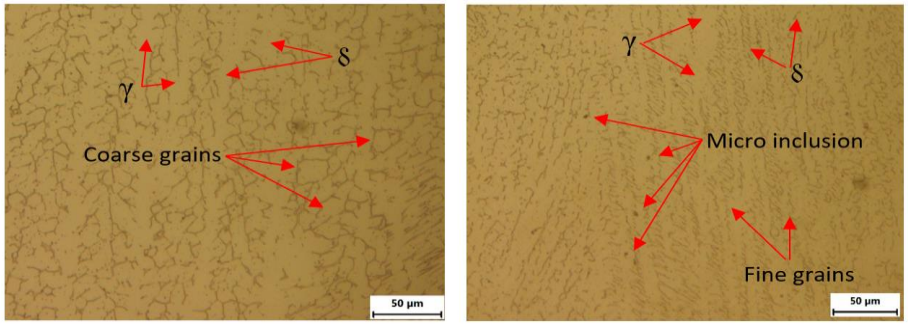

(a) (b)

Fig. 5. Magnified optical microscopic image of (a) non-inoculated (b) inoculant Al_2O_3 of WAAM component

Upon completion of the static tensile testing, the scanning electron microscope (SEM) was deployed to determine the effect of inoculation on morphological fracture surfaces. Figure 6(a) and 6(b) depicts the SEM images of a horizontal fracture surface of non-inoculated at different magnification. Whereas, inoculated specimens are shown in Figure 6(c) and 6(d). The images show that the WAAM structure fabricated by SS308LSi exhibited excellent non-porous ductile rupture failure with a clear appearance of numerous dimples distributed on all surfaces. This result is supported by Chaudhari *et al.,* [26] who found that the existence of a greater number of dimples adjacent to each other demonstrates that the multi-walled structure sample components have excellent ductility which implies a higher strength. Moreover, the failure occurred in a ductile manner as a result of the micro-void nucleation, growth and coalescence mechanism to form a continuous fracture path. In addition, the plastic deformation was sufficient during tensile testing by referring to the tear edges formed around the dimples. Based on analysis of the images, the specimens of fracture morphologies exhibited existence of dimples with homogeneous distribution as a result of ductile failure.

However, there are obvious visible depth and dimple size comparisons between non-inoculated shown in Figure 6(b) and inoculant Al_2O_3 ceramic particle deposition parts depicted in Figure 6(d). It is revealed that the existence of significant quantities of dimples as well as deeper dimple size was observed after the introduction of inoculant Al_2O_3 ceramic particles. This is mainly due to the dimple's characteristics will influence the result of tensile strength. Wang *et al.,* [27] reported similar behaviour in that the dimple characteristics are an indicator of ductile rupture for instance, a deeper dimple signifies a higher tensile strength. Prasanna *et al.,* [28] discovered that bigger and deeper dimples of fracture samples lead to significant UTS and EL in WAAM components manufactured using stainless steel ER308L deposited via the GMAW- CMT approach. Furthermore, they acted as dimple nucleation sites in the as-deposited wall during the tensile fracture. It is more possible for these areas to nucleate cracks. The result also shows that inclusions are globular or nearly globular in shape.

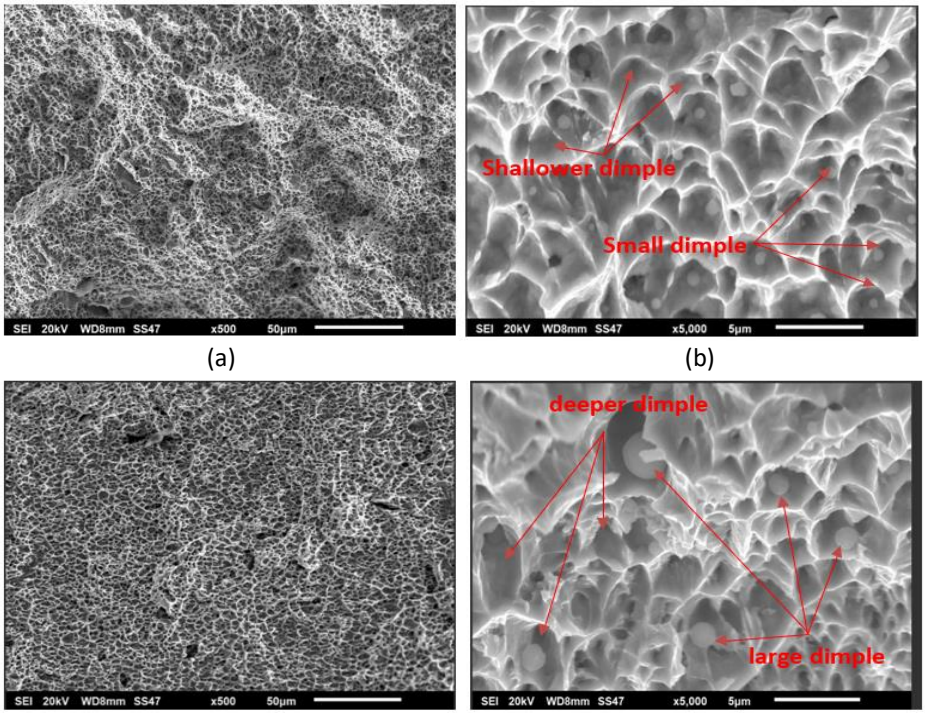

Fig. 6. Fracture surface WAAM sample (a-b) non-inoculated (c-d) inoculated Al_2O_3 ceramic particle

Additionally, the Energy-dispersive spectroscopy (EDS) analysis was performed. The micro inclusions representing an atomic fraction of Al and O was the main Al_2O_3 ceramic particle inoculant element. The matrix could be categorized as in situ Al_2O_3 particles inclusion with scattered in the microstructure marked by spectrum 1 as shown in Figure 7. The presence of the black spherical oxide inclusion improves the sample's strength. Moreover, as nanosized inclusion with low content are present in WAAM structure and is evenly distributed and well bonded with the matrix, elongation tends to remain unaffected. However, it can also be a cause for fracture source and lower the sample's plasticity [38].

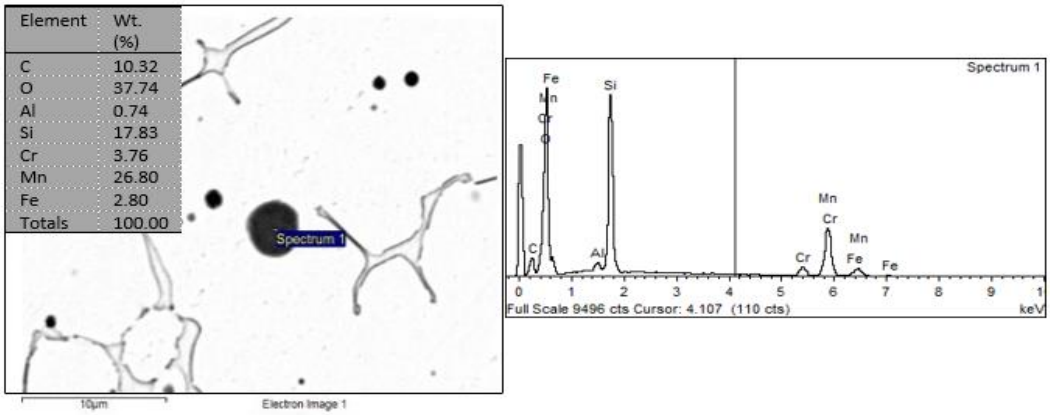

Fig. 7. Element composition of the selected point micro inclusion for inoculated Al_2O_3

3.2 Tensile Strength

Tensile strength is an essential property of a material to resist tearing due to tension and determines its mechanical performance. Optimizing the tensile properties also leads to excellence in the plastic effect flow process around the tool pins. Figure 8 shows the comparative elongation and UTS effect between non-inoculated and inoculant Al_2O_3 ceramic particle results deposited using SS308LSi welding wire of WAAM wall structure. Based on the graph, the lower result of non–inoculated clearly shows WAAM structure show a lower tensile strength that indicates poor mechanical properties as depicted in Figure 8(a). In the absence of Alumina-inoculated, UTS values in the WAAM deposition (X-direction) are 538 MPa for the top side, 535 MPa at the middle side and 525MPa attained on the bottom side. Meanwhile, the UTS values of samples inoculated with Al_2O_3 ceramic particles exhibit a tremendously increasing value for all top, middle and bottom sides which are 560MPa, 551MP and 550Mpa respectively. Hence, the overall UTS increased by 4%, 3% and 5% on all sides.

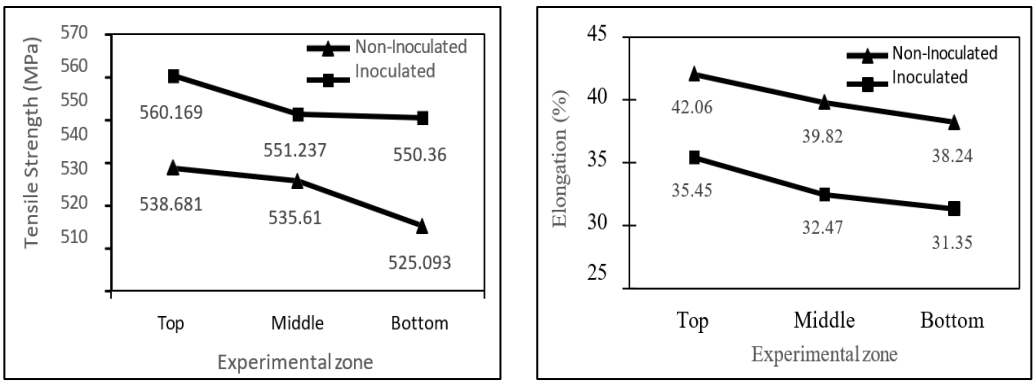

(a) (b)

Fig. 8. (a) Ultimate tensile strength (b) elongation

Additionally, when a tensile force is applied to the WAAM sample, dislocations acquire around the particles and stress concentration arises due to movement restriction established by Al_2O_3 particles. Micropores will form at the interfaces between Al_2O_3 ceramic particles and the stainless steel 308LSi matrix. Afterward, the continuous dislocations will then be directed into the micropores, causing the pores to develop. As a result, the matrix between bordering micropores undergoes continual plastic deformation and internal necking thus ending with dimple formation. Ultimately, the micropores unite, resulting in microcracks formation, which continues to stretch and expand until the sample fails [29]. This process contributed to the occurrence of deep and large dimples size as depicted in Figure 6(d) thus correlating to the result in higher tensile strength as shown in Figure 8(a).

Based on a fracture behaviour test in a study entitled in–situ synthesis of an Al–based composite reinforced with nanometric γ– Al_2O_3 and submicron AlB2 particles, Gao *et al.,* [30] discovered that dimples in a deep size are due to the presence of Al_2O_3 ceramic particles, therefore it improves fracture of EL and RT sample, respectively. Furthermore, consistent behaviour of mechanical properties demonstrated the superiority of deposited components in a variety of applications. This study reveals that the introduction of inoculant Al_2O_3 ceramic particles during SS308LSi deposition has significantly increased the strength of WAAM components with successive increment in the mechanical properties of the structures compared with the non-inoculated structures.

However, this improvement in mechanical properties came at the expense of low elongation. Based on the graph, the elongation to fracture of Al_2O_3 ceramic particles is mainly owing to the agglomeration of alumina particles due to particles having higher surface energy and some particles

are not wettable with the matrix. In addition, since there is a powerful bond between Al and impurity elements such as O in the Fe-Al-O systems of molten steel, Al_2O_3 high melting point inclusion tends to form. Therefore, in this condition, the agglomerates occur due to weakly bonded particles that stick together under van der Waals forces [10]. The results were in line with the reasonable agreement reported by Liu *et al.,* [31].

It can be concluded that the correlation between mechanical properties and microstructure can be further tailored via the addition of Al_2O_3 ceramics inoculant. On the other hand, tensile strength relies on the metallurgical behaviour of a metal that undergoes phase changes due to the solidification process. Thus, a very fine grain structure or smaller grain size is desired to increase tensile strength properties. It is found that with the introduction of Al_2O_3 ceramics inoculants that dispersed in the matrix during solidification, the maximum tensile strength can be achieved due to microstructural refinement. In addition, the microstructure and mechanical properties of WAAM structure may be influenced by the presence of elemental oxygen and/or oxide particles due to the restrictions of dislocation movements and grain boundaries [44].

Furthermore, Table 3 shows the comparison of ultimate tensile properties of the previous studies using stainless steel 308, 308L and 308 LSi, ASTM A479 as well as industrial requirement standards for forging applications. The result is filtered only focusing on the horizontal direction of the deposition strategy. The result reveals that the effect of the introduction of an inoculant Al_2O_3 ceramic particle during deposition of WAAM wall had significantly improved the tensile strength of the material compared to other studies. The results show better properties of the wrought 308L stainless steel and ASTM A479 ER308L stainless steel can be obtained.

Table 3
Comparison of ultimate tensile properties of SS308 by various AM

Deposition method	Material	Tensile strength, (MPa)	Ref
Annealed ASTM A479	Stainless Steel ER308	≥515	[32]
Industrial standards for stainless steel	-	450	[33]
WAAM	Stainless Steel 308L	504.93	[34]
WAAM	Stainless Steel 308L	557.91	[35]
Laser-based AM	Stainless Steel 308LSi	548	[36]
WAAM	Stainless Steel 308LSi	560	[this study]

3.3 Future Scope for Research

Future research may improve the accuracy and flexibility of the WAAM process in restoring used products. This is to ensure the same quality, functionality and lifetime extension as well as fast service restoration especially in critical components by remanufacturing process can be a success. Therefore, focus on the improvement of material properties and surface finish is crucial and has gained researchers' interest. Introduction of Al_2O_3 ceramic particles can refine the grain size of WAAM components by varying the amount of Al_2O_3 ceramic inoculants and controlling heat input which can be explored more extensively through further experiments.

4. Conclusions

In this study, an innovative Stainless Steel 308LSi WAAM wall structure was developed with the introduction of Al_2O_3 ceramic alumina particles as inoculant during the deposition process. The effect of Al_2O_3 ceramic alumina particles was investigated and compared with non-inoculated structure

using microstructures analysis, microscopic characterization and mechanical properties. Thus, the following conclusion was drawn:

i. The tensile properties of the Stainless Steel WAAM 308LSi wall structure inoculated with Al2O3 ceramic alumina particles were outstandingly improved compared to the non-inoculated sample. The ultimate tensile strength in the deposition direction increased from 538 MPa and 525 MPa to 560 MPa and 550MPa, an increase of 22 MPa (4%) and 25 MPa (5%), respectively. The results obtained showed far better strength than the industrial standard for stainless steel (450 MPa). The refined grain structure due to the introduction of inoculant Al2O3 ceramic alumina contributed to this improvement.
ii. The coarse columnar grain was refined to a more homogeneous fine grain structure after the introduction of Al2O3 ceramic alumina due to the stimulating crystal grain nucleation which resulted in a uniform and refined grain structure.
iii. SEM analysis of the fracture surface morphologies of tensile parts revealed the presence of inclusion agglomeration of alumina particles due to impurity elements such as O in the Fe-Al-O systems of molten steel with a uniform even distribution. The occurrence of more dimples closes to one another verified the excellent ductility of sample components.
iv. The results indicate that the presence of Al2O3 ceramic alumina particles in WAAM structure can be applied in the deposited multi-walled structure of Stainless Steel 308LSi for broad applications in industry including remanufacturing purposes.

Acknowledgment
This research was funded by the Ministry of Higher Education (MOHE), Malaysia under Geran Konsortium Kecemerlangan Penyelidikan (JPT(BPKI)1000/016/018/25(52)) and other support from Universiti Teknikal Malaysia Melaka (UTeM).

References

[1] Yildiz, Ahmet Suat, Kemal Davut, Barış Koc and Oguzhan Yilmaz. "Wire arc additive manufacturing of high-strength low alloy steels: study of process parameters and their influence on the bead geometry and mechanical characteristics." *The International Journal of Advanced Manufacturing Technology* 108 (2020): 3391-3404. https://doi.org/10.1007/s00170-020-05482-9
[2] Huang, Wenjia, Qian Wang, Ninshu Ma and Houichi Kitano. "Distribution characteristics of residual stresses in typical wall and pipe components built by wire arc additive manufacturing." *Journal of Manufacturing Processes* 82 (2022): 434-447. https://doi.org/10.1016/j.jmapro.2022.08.010
[3] Chaudhari, Rakesh, Nipun Parikh, Sakshum Khanna, Jay Vora and Vivek Patel. "Effect of multi-walled structure on microstructure and mechanical properties of 1.25 Cr-1.0 Mo steel fabricated by GMAW-based WAAM using metal-cored wire." *Journal of Materials Research and Technology* 21 (2022): 3386-3396. https://doi.org/10.1016/j.jmrt.2022.10.158
[4] Vora, Jay, Heet Parmar, Rakesh Chaudhari, Sakshum Khanna, Mikesh Doshi and Vivek Patel. "Experimental investigations on mechanical properties of multi-layered structure fabricated by GMAW-based WAAM of SS316L." *Journal of materials research and technology* 20 (2022): 2748-2757. https://doi.org/10.1016/j.jmrt.2022.08.074
[5] Standard, A. S. T. M. "Standard terminology for additive manufacturing technologies." *ASTM International F2792-12a* 46 (2012): 10918-10928.
[6] Ahn, Dong-Gyu. "Directed energy deposition (DED) process: state of the art." *International Journal of Precision Engineering and Manufacturing-Green Technology* 8, no. 2 (2021): 703-742. https://doi.org/10.1007/s40684-020-00302-7
[7] Cunningham, C. R., J. M. Flynn, Alborz Shokrani, Vimal Dhokia and S. T. Newman. "Invited review article: Strategies and processes for high quality wire arc additive manufacturing." *Additive Manufacturing* 22 (2018): 672-686. https://doi.org/10.1016/j.addma.2018.06.020

[8] Raut, Laukik P., R. V. Taiwade and Ankit Agarwal. "Investigation of microstructural and corrosion behavior of 316LSi structure developed by wire arc additive manufacturing." *Materials Today Communications* 35 (2023): 105596. https://doi.org/10.1016/j.mtcomm.2023.105596

[9] Farias, Francisco Werley Cipriano, Valdemar R. Duarte, Igor Oliveira Felice, Joao da Cruz Payao Filho, Norbert Schell, Emad Maawad, J. A. Avila *et al.,* "In situ interlayer hot forging arc-based directed energy deposition of Inconel® 625: process development and microstructure effects." *Additive Manufacturing* 66 (2023): 103476. https://doi.org/10.1016/j.addma.2023.103476

[10] Liu, Jin, Jili Liu, Han Wang, Changlang Jiang and Wei Huang. "Research on adding nano-SiC reinforced wire arc additive manufacturing stainless steel." *Journal of Materials Engineering and Performance* 31, no. 6 (2022): 4945-4954. https://doi.org/10.1007/s11665-021-06574-7

[11] Ghaffari, Mahya, Alireza Vahedi Nemani, Sajad Shakerin, Mohsen Mohammadi and Ali Nasiri. "Grain refinement and strengthening of PH 13-8Mo martensitic stainless steel through TiC/TiB2 inoculation during wire arc additive manufacturing." *Materialia* 28 (2023): 101721. https://doi.org/10.1016/j.mtla.2023.101721

[12] Jiang, Xing, Xinjie Di, Chengning Li, Dongpo Wang and Wenbin Hu. "Improvement of mechanical properties and corrosion resistance for wire arc additive manufactured nickel alloy 690 by adding TiC particles." *Journal of Alloys and Compounds* 928 (2022): 167198. https://doi.org/10.1016/j.jallcom.2022.167198

[13] Rodrigues, Tiago A., V. R. Duarte, David Tomás, Julian A. Avila, J. D. Escobar, Emma Rossinyol, N. Schell, Telmo G. Santos and J. P. Oliveira. "In-situ strengthening of a high strength low alloy steel during Wire and Arc Additive Manufacturing (WAAM)." *Additive manufacturing* 34 (2020): 101200. https://doi.org/10.1016/j.addma.2020.101200

[14] Jandaghi, Mohammad Reza, Hesam Pouraliakbar, Sang Hun Shim, Vahid Fallah, Sun Ig Hong and Matteo Pavese. "In-situ alloying of stainless steel 316L by co-inoculation of Ti and Mn using LPBF additive manufacturing: Microstructural evolution and mechanical properties." *Materials Science and Engineering: A* 857 (2022): 144114. https://doi.org/10.1016/j.msea.2022.144114

[15] Yuan, Tao, Xuelei Ren, Shujun Chen and Xiaoqing Jiang. "Grain refinement and property improvements of Al–Zn–Mg–Cu alloy by heterogeneous particle addition during wire and arc additive manufacturing." *Journal of Materials Research and Technology* 16 (2022): 824-839. https://doi.org/10.1016/j.jmrt.2021.12.049

[16] Kennedy, Jacob R., Alec E. Davis, A. E. Caballero, Stewart Williams, E. J. Pickering and P. B. Prangnell. "The potential for grain refinement of Wire-Arc Additive Manufactured (WAAM) Ti-6Al-4V by ZrN and TiN inoculation." *Additive Manufacturing* 40 (2021): 101928. https://doi.org/10.1016/j.addma.2021.101928

[17] Li, Shuang-Shuang, Feng Qiu, Hong-Yu Yang, Shuan Liu, Tian-Shu Liu, Liang-Yu Chen and Qi-Chuan Jiang. "Strengthening of dislocation and precipitation for high strength and toughness casting Al–Zn–Mg–Cu alloy via trace TiB2+ TiC particles." *Materials Science and Engineering: A* 857 (2022): 144107. https://doi.org/10.1016/j.msea.2022.144107

[18] Jin, Peng, Yibo Liu and Qingjie Sun. "Evolution of crystallographic orientation, columnar to equiaxed transformation and mechanical properties realized by adding TiCps in wire and arc additive manufacturing 2219 aluminum alloy." *Additive Manufacturing* 39 (2021): 101878. https://doi.org/10.1016/j.addma.2021.101878

[19] Zhang, Jinbao, Jun He, Jianhang Feng, Ming Xu, Ping Zhang, Cuixin Chen and Huifen Peng. "On the WAAM characteristics of oxide-modified H13 solid wire by MAG process." *Journal of Materials Research and Technology* 25 (2023): 2324-2332. https://doi.org/10.1016/j.jmrt.2023.06.106

[20] Paul, Amrit Raj, Avinash Mishra, Manidipto Mukherjee and Dilpreet Singh. "Stainless steel to aluminium joining by interfacial doping with Al2O3 powder in wire arc direct energy deposition process." *Materials Letters* 330 (2023): 133349. https://doi.org/10.1016/j.matlet.2022.133349

[21] Kumar, A. Varun, A. S. Selvakumar, K. Balachandar, A. Waseem Ahmed and A. Yashar Arabath. "Correlation between material properties and free vibration characteristics of TIG and laser welded stainless steel 304 reinforced with Al2O3 microparticles." *Engineering Science and Technology, an International Journal* 24, no. 5 (2021): 1253-1261. https://doi.org/10.1016/j.jestch.2021.01.017

[22] Olshanskaya, Tatyana, Dmitry Trushnikov, Alyona Dushina, Artur Ganeev, Alexander Polyakov and Irina Semenova. "Microstructure and properties of the 308LSi austenitic steel produced by plasma-MIG deposition welding with layer-by-layer peening." *Metals* 12, no. 1 (2022): 82. https://doi.org/10.3390/met12010082

[23] Koli, Yashwant, S. Aravindan and P. V. Rao. "Influence of heat input on the evolution of δ-ferrite grain morphology of SS308L fabricated using WAAM-CMT." *Materials Characterization* 194 (2022): 112363. https://doi.org/10.1016/j.matchar.2022.112363

[24] Saluja, Rati and K. M. Moeed. "Experimental Investigation of Solidification-Mode and Response Surface Modeling of Ferrite-Content in Grade 304L Pulse GMA Welded Plates." *Materials Today: Proceedings* 18 (2019): 3876-3890. https://doi.org/10.1016/j.matpr.2019.07.327

[25] Li, Haonan, Kui Wang, Gaopeng Xu, Haiyan Jiang, Qudong Wang and Yingxin Wang. "Effective inhibition of anomalous grain coarsening in cast AZ91 alloys during fast cooling via nanoparticle addition." *Journal of Magnesium and Alloys* (2021).
[26] Chaudhari, Rakesh, Nipun Parikh, Sakshum Khanna, Jay Vora and Vivek Patel. "Effect of multi-walled structure on microstructure and mechanical properties of 1.25 Cr-1.0 Mo steel fabricated by GMAW-based WAAM using metal-cored wire." *Journal of Materials Research and Technology* 21 (2022): 3386-3396. https://doi.org/10.1016/j.jmrt.2022.10.158
[27] Wang, Tingting, Yuanbin Zhang, Zhihong Wu and Chuanwei Shi. "Microstructure and properties of die steel fabricated by WAAM using H13 wire." *Vacuum* 149 (2018): 185-189. https://doi.org/10.1016/j.vacuum.2017.12.034
[28] Prasanna Nagasai, Bellamkonda, Sudersanan Malarvizhi and Visvalingam Balasubramanian. "A study on wire arc additive manufacturing of 308L austenitic stainless steel cylindrical components: optimisation, microstructure and mechanical properties." *Proceedings of the Institution of Mechanical Engineers, Part B: Journal of Engineering Manufacture* 237, no. 9 (2023): 1391-1404. https://doi.org/10.1177/09544054221129471
[29] Wang, Changji, He Huang, Shizhong Wei, Laiqi Zhang, Kunming Pan, Xiaonan Dong, Liujie Xu *et al.,* "Strengthening mechanism and effect of Al2O3 particle on high-temperature tensile properties and microstructure evolution of W–Al2O3 alloys." *Materials Science and Engineering: A* 835 (2022): 142678. https://doi.org/10.1016/j.msea.2022.142678
[30] Gao, Tong, Lingyu Liu, Guiliang Liu, Sida Liu, Chunxiao Li, Mengyu Li, Kai Zhao, Mengxia Han, Yuying Wu and Xiangfa Liu. "In–situ synthesis of an Al–based composite reinforced with nanometric γ–Al2O3 and submicron AlB2 particles." *Journal of Alloys and Compounds* 920 (2022): 165985. https://doi.org/10.1016/j.jallcom.2022.165985
[31] Liu, Kun, Xiaoqing Jiang, Shujun Chen, Tao Yuan and Zhaoyang Yan. "Effect of SiC addition on microstructure and properties of Al–Mg alloy fabricated by powder and wire cold metal transfer process." *Journal of Materials Research and Technology* 17 (2022): 310-319. https://doi.org/10.1016/j.jmrt.2022.01.014
[32] Li, Yajing, Ying Luo, Jianghua Li, Danrong Song, Bin Xu and Xu Chen. "Ferrite formation and its effect on deformation mechanism of wire arc additive manufactured 308 L stainless steel." *Journal of Nuclear Materials* 550 (2021): 152933. https://doi.org/10.1016/j.jnucmat.2021.152933
[33] Wu, Wei, Jiaxiang Xue, Leilei Wang, Zhanhui Zhang, Yu Hu and Changwen Dong. "Forming process, microstructure and mechanical properties of thin-walled 316L stainless steel using speed-cold-welding additive manufacturing." *Metals* 9, no. 1 (2019): 109. https://doi.org/10.3390/met9010109
[34] Mai, Dinh Si and Henri Paris. "Influences of the compressed dry air-based active cooling on external and internal qualities of wire-arc additive manufactured thin-walled SS308L components." *Journal of Manufacturing Processes* 62 (2021): 18-27. https://doi.org/10.1016/j.jmapro.2020.11.046
[35] Mai, Dinh Si. "Microstructural and mechanical characteristics of 308L stainless steel manufactured by gas metal arc welding-based additive manufacturing." *Materials Letters* 271 (2020): 127791. https://doi.org/10.1016/j.matlet.2020.127791
[36] Abioye, T. E., A. Medrano-Tellez, P. K. Farayibi and P. K. Oke. "Laser metal deposition of multi-track walls of 308LSi stainless steel." *Materials and Manufacturing Processes* 32, no. 14 (2017): 1660-1666. https://doi.org/10.1080/10426914.2017.1292034
[37] Niu, Fangyong, Weiming Bi, Kaijun Zhang, Xiong Sun, Guangyi Ma and Dongjiang Wu. "Additive manufacturing of 304 stainless steel integrated component by hybrid WAAM and LDED." *Materials Today Communications* 35 (2023): 106227. https://doi.org/10.1016/j.mtcomm.2023.106227
[38] Zhai, Wengang, Wei Zhou and Sharon Mui Ling Nai. "Grain refinement of 316L stainless steel through in-situ alloying with Ti in additive manufacturing." *Materials Science and Engineering: A* 840 (2022): 142912. https://doi.org/10.1016/j.msea.2022.142912